

## Circulating Neonatal Nav1.5 (nNav1.5) Antigen and Anti-nNav1.5 Antibodies as Potential Biomarkers for Breast Cancer Metastasis

(Peredaran Antigen dan Antibodi Neonatal Nav1.5 (nNav1.5) Sebagai Penanda Biologi Berpotensi untuk Metastasis Kanser Payu Dara)

HARISHINI RAJARATINAM<sup>1</sup>, NUR SYAHMINA RASUDIN<sup>1</sup>, MAYA MAZUWIN YAHYA<sup>2,3</sup>, WAN ZAINIRA WAN ZAIN<sup>2</sup>, SABREENA SAFUAN<sup>1</sup>, NURUL ASMA-ABDULLAH<sup>1</sup>, NOOR FATMAWATI MOKHTAR<sup>4</sup> & WAN EZUMI MOHD FUAD<sup>1\*</sup>

<sup>1</sup>*School of Health Sciences, Health Campus, Universiti Sains Malaysia, 16150 Kubang Kerian, Kelantan Darul Naim, Malaysia*

<sup>2</sup>*Department of Surgery, School of Medical Sciences, Health Campus, Universiti Sains Malaysia, 16150 Kubang Kerian, Kelantan Darul Naim, Malaysia*

<sup>3</sup>*Breast Cancer Awareness and Research (BestARi) Unit, Hospital Universiti Sains Malaysia, 16150 Kubang Kerian, Kelantan Darul Naim, Malaysia*

<sup>4</sup>*Institute for Research in Molecular Medicine (INFORMM), Health Campus, Universiti Sains Malaysia, 16150 Kubang Kerian, Kelantan Darul Naim, Malaysia*

Received: 4 January 2022/Accepted: 14 March 2022

### ABSTRACT

Neonatal Nav1.5 (nNav1.5) has been known to potentiate breast cancer (BCa) metastasis. The detection of anti-nNav1.5 antibodies (anti-nNav1.5-Ab) reflects the immunogenicity of nNav1.5. However, the presences of circulating nNav1.5 antigen and anti-nNav1.5-Ab in the context of BCa metastasis have not been explored yet. Therefore, the study has attempted to conduct such an investigation using both blood samples from 4T1 orthotopic mice and BCa patients. In the preclinical study, forty female BALB/c mice were divided into three groups: 4T1 orthotopic BCa mice ( $n=17$ ), control mice ( $n=20$ ) and positive control mice ( $n=3$ ). After tumour development, the mice were sacrificed to obtain target organs, whole blood, and serum. Histopathology, cytokine analyses, real-time PCR, and indirect ELISA were performed. Histopathology and cytokine analyses showed the establishment of metastasis in 4T1 orthotopic mice. The concentration of vascular endothelial growth factor (VEGF) was significantly higher in the 4T1 orthotopic mice ( $P<0.0001$ \*\*\*\*). Circulating nNav1.5 antigen and anti-nNav1.5-Ab were detected in 4T1 orthotopic mice, using real-time PCR and indirect ELISA, respectively. Furthermore, there was an inverse relationship between anti-nNav1.5-Ab and the total metastatic foci ( $P=0.0485^*$ ,  $r=-0.7306$ ). In the clinical study, 32 BCa patients were grouped based on their stages: early-invasive ( $n=15$ ) and advanced ( $n=17$ ) stages. Approximately 3 mL of blood was withdrawn, and only indirect ELISA was conducted. The clinical study showed that BCa patients of advanced-stages portrayed higher expression of anti-nNav1.5-Ab compared to early stages of BCa ( $P=0.0110^*$ ). In conclusion, the detection of nNav1.5 antigen and anti-nNav1.5-Ab was consistent with the presence of BCa metastasis.

Keywords: Breast cancer patients; *in vivo*; metastasis; Neonatal Nav1.5; orthotopic; 4T1

### ABSTRAK

Neonatal Nav1.5 (nNav1.5) telah dikenal pasti mampu mendorong metastasis kanser payu dara. Pengesanan antibodi anti-nNav1.5 (anti-nNav1.5-Ab) mencerminkan nNav1.5 bersifat imunogen. Walau bagaimanapun, peredaran antigen neonatal Nav1.5 dan anti-nNav1.5-Ab di dalam konteks kanser payu dara (KP) yang bermetastasis masih belum dikaji. Oleh itu, penyelidikan ini telah dijalankan untuk mengkaji perkara tersebut dengan menggunakan sampel darah daripada tikus ortotopik 4T1 dan pesakit KP. Dalam kajian praklinikal, empat puluh ekor tikus BALB/c betina dibahagikan kepada tiga kumpulan: tikus KP ortotopik 4T1 ( $n=17$ ), tikus kawalan ( $n=20$ ) dan tikus kawalan positif ( $n=3$ ). Selepas perkembangan tumor, tikus dikorbankan untuk mendapatkan organ sasaran, darah dan serum. Histopatologi, analisis

sitokin, PCR masa-nyata dan ELISA tidak langsung telah dijalankan. Histopatologi dan analisis sitokin menunjukkan berlakunya pembentukan metastasis pada tikus ortotopik 4T1. Kepekatan faktor pertumbuhan endothelium vaskular (VEGF) adalah lebih tinggi secara signifikan pada tikus ortotopik 4T1 ( $P < 0.0001$ \*\*\*\*). Peredaran antigen nNav1.5 dan anti-nNav1.5-Ab telah dikesan pada tikus ortotopik 4T1, masing-masing menggunakan PCR masa-nyata dan ELISA tak langsung. Tambahan pula, terdapat hubung kait songsang antara anti-nNav1.5-Ab dan jumlah fokus metastatik ( $P = 0.0485^*$ ,  $r = -0.7306$ ). Melalui kajian klinikal pula, 32 pesakit KP telah dikumpulkan berdasarkan peringkat kanser: peringkat awal invasif ( $n = 15$ ) dan lanjutan ( $n = 17$ ). Sebanyak, 3 mL darah telah diambil dan hanya ELISA tak langsung telah dijalankan. Kajian klinikal ini membuktikan bahawa pesakit KP peringkat lanjutan menunjukkan ekspresi anti-nNav1.5-Ab yang lebih tinggi berbanding pesakit KP peringkat awal ( $P = 0.0110^*$ ). Kesimpulannya, pengesanan antigen nNav1.5 dan anti-nNav1.5-Ab adalah konsisten dengan kehadiran metastasis KP.

Kata kunci: *in vivo*; metastasis; neonatal Nav1.5; ortotopik; pesakit kanser payu dara; 4T1

## INTRODUCTION

The involvement of voltage-gated sodium channels (VGSCs) in the progression of various types of cancer has been highlighted over the years in various settings (Diaz et al. 2007; Gao et al. 2010; Onganer & Djamgoz 2005). The VGSCs are heteromeric membrane complexes, made of a pore-forming alpha ( $\alpha$ ) subunit and four non-pore-forming beta ( $\beta$ ) subunits. In general, the VGSC  $\alpha$ -subunit family consists of nine members, which are Nav1.1-Nav1.9 (Brackenbury 2012; Catterall 2000; Patel & Brackenbury 2015). Nav1.5 channel, particularly, conducts an inward sodium ion ( $\text{Na}^+$ ) current, which determines the  $\text{Na}^+$  influx that functions to depolarise the cell membrane during the upstroke of the cardiac action potential. The function of Nav1.5 is essential in the initiation and conduction of cardiac action potentials (Rook et al. 2012). A ground-breaking study by Roger et al. (2003) showed a unique fast inward  $\text{Na}^+$  current in highly metastatic breast cancer (BCa) cells, MDA-MB-231. The study initiated the pathway towards future studies that showed interest in studying the relationship between the role of  $\text{Na}^+$  current in prompting BCa invasion and metastasis. A study by Nelson et al. (2015) showed the functional role of Nav1.5 in enhancing the dissemination of BCa metastasis. Recently, Yang et al. (2020) discovered that the activation of Rac1 by Nav1.5 channel stimulated cell migration in BCa cells.

However, a considerable number of research suggested that the neonatal isoform of Nav1.5 plays a more significant role in potentiating BCa metastasis rather than the adult form of Nav1.5. The deviant expression of neonatal Nav1.5 (nNav1.5), an alternative splice variant of Nav1.5 ( $\alpha$ -subunit of VGSC) in the development of metastasis in BCa, has gained incredible attention over the years among researchers (Brackenbury et al. 2007; Chioni et al. 2005; Fraser et al. 2005). The molecular differences between these two isoforms

include the position of Nav1.5 (3') and nNav1.5 (5') on exon six and the seven amino acid changes in the sequence of nNav1.5 protein compared to Nav1.5. The location of alternative splicing is the segment 3-4 (S3-4) regions of the domain 1 (D1) of the protein, including the extracellular S3-4 linker (Onkal et al. 2008). Due to the electrophysiological changes contributed from the splicing, the charge reversal in nNav1.5 modified the kinetics of the channel, which results in the prolonged resultant current thus, causing an increased intracellular  $\text{Na}^+$  influx (Onkal et al. 2008).

The increased influx of  $\text{Na}^+$  via the sodium channel leads to an accumulation of hydrogen ions ( $\text{H}^+$ ), causing extracellular acidification adjacent to the plasma membrane. The low pH contributes to the activation of cysteine cathepsins, which degrades the integrity of the extracellular membrane (ECM), favouring the invasion of cancerous cells (Gillet et al. 2009). The degradation of the ECM is necessary for the dissociation, migration, and invasion of the BCa cells into the circulation system (lymphatic and blood systems).

The expression of nNav1.5 in BCa metastasis and aggressiveness have been extensively carried out via *in vitro* studies (Kamarulzaman et al. 2017; Luo et al. 2020; Yang et al. 2012). Brackenbury et al. (2007) reported the suppression of nNav1.5 via the introduction of RNA interference and NESO-pAb, which indicated that the protein is responsible for potentiating the invasive behaviour of MDA-MB-231 human BCa cells. *In vivo* expression of nNav1.5 in human BCa biopsy samples was first mentioned by Fraser et al. (2005), whereby it was postulated that the expression of nNav1.5 (sequenced from Nav1.5 positive samples) in the biopsy samples was related to the presence of lymph node metastasis. Another example of a tissue-based study was by Yamaci et al. (2017), where the immunoreactivity of nNav1.5 was significantly higher in BCa tissue. It is

important to note that these past studies have only focused on detecting nNav1.5 in tissues and cell lines.

In our previous work, we have studied the varying expression of anti-nNav1.5-Ab in the serum of BCa patients with respect to their treatment status (Rajaratnam et al. 2021). It was our first published paper on the immunogenicity of nNav1.5 and the detection of anti-nNav1.5-Ab in the serum. From the clinical study, we found that pre-treatment BCa patients exhibited an upregulated expression of anti-nNav1.5-Ab compared to their counterparts. In addition, those patients also displayed an increase in the pro-inflammatory cytokines that mirrors the progression of BCa metastasis. However, the previous study did not focus on the in-depth existence of BCa metastasis as the BCa patients were not grouped based on their cancer stages at diagnosis. The study also lacked histological evidence that may have provided more information on the progression of BCa metastasis. Such limitation was tackled in the present study using *in vivo* model, which added extensive knowledge on the relationship between the expressions of nNav1.5 and anti-nNav1.5-Ab with BCa metastasis.

First of its kind, we have attempted to demonstrate the presence of circulating nNav1.5 antigen in blood, with respect to BCa metastasis, via animal study. On the other hand, the presence of anti-nNav1.5-Ab in serum samples has been previously demonstrated in our published study. However, the expression of these antibodies concerning to BCa metastasis was not directly studied. Therefore, using both animal models and samples from BCa patients (with varying BCa stages), we have extended our study to incorporate the relationship between the anti-nNav1.5-Ab and BCa metastasis. However, the apparent limitation of the animal model is that it does not represent the broad spectrum of varying stages of BCa metastasis. Therefore, a clinical study was included to highlight the pattern of anti-nNav1.5-Ab expression in different stages of human BCa. The following sections, materials and methods, results, and discussion will be classified into two major subtopics; study I: preclinical animal study using 4T1 orthotopic BCa mice model and study II: a clinical study using serum samples from BCa patients.

## MATERIALS AND METHODS

### STUDY I: PRECLINICAL ANIMAL STUDY USING 4T1 ORTHOTOPIC BCA MICE MODEL

#### SAMPLE SIZE, LOCATION OF STUDY, AND ETHICAL APPROVAL

A total of 40 female BALB/c mice (around 20-23 g), aged between five to six weeks were utilised in this study. The

BALB/c mice were randomly divided into three groups: normal control mice ( $n=20$ ), 4T1 orthotopic mice models ( $n=17$ ) and positive control sera group ( $n=3$ ). The animal study was conducted at the Animal Research and Service Centre (ARASC), Universiti Sains Malaysia (USM), Health Campus, Kubang Kerian, Kelantan, Malaysia. Ethical approval for the animal study was granted by the USM Institutional Animal Care and Use Committee (USM IACUC) (approval no. USM/IACUC/2018/(113)(934). All 40 mice were housed in a controlled environment of standard laboratory conditions and were provided with a standard pellet diet and water *ad libitum*. The animal study was performed under the supervision of a veterinarian.

#### CELL CULTURE OF 4T1 MURINE MAMMARY CELL LINE

4T1 mammary cell line (passage 8) purchased from the American Type Culture Collection (ATCC) was revived from cryovial storage. It was subsequently cultured in complete media, Dulbecco's Modified Eagle Medium (DMEM) (*Gibco*) supplied with 10% of fetal bovine serum (FBS) (*Gibco*) and 1% of antibiotics, penicillin, and streptomycin (*Gibco*). Upon reaching passage 10, the grown cells that have reached 90-100% confluency were harvested using 0.25% trypsin (*Gibco*) for the preparation of 4T1 orthotopic injection.

#### PREPARATION OF 4T1 ORTHOTOPIC INJECTION FOR THE DEVELOPMENT OF 4T1 TUMOUR

Approximately,  $1 \times 10^5$  number of cells were isolated from the suspension, for the preparation of the 4T1 orthotopic injection. The volume taken from the cell suspension was diluted in phosphate buffer saline (PBS) (pH: 7.4) and loaded into a 1 mL syringe attached to a 27 G needle. The procedure was adapted from a previous study (Pulaski & Ostrand-Rosenberg 2000).

#### DEVELOPMENT OF 4T1 ORTHOTOPIC MICE MODELS

Approximately, 200  $\mu$ L of 4T1 orthotopic injection was introduced subcutaneously at the 3<sup>rd</sup> mammary fat pad of the BALB/c mice. The procedure was adapted from previous studies (Paschall & Liu 2016). For the control group, a similar volume of sterile PBS alone (without 4T1 cells) was introduced at the similar site. The volume of the tumour was monitored for 6 weeks (42 days) using a vernier caliper. The diameter and width were recorded, and the volume of the tumour was calculated using the formula:  $0.52 \times \text{width}^2 \times \text{diameter}$  (Sauter et al. 2000). On day 43, both 4T1 and control mice groups were sacrificed via decapitation after being anaesthetised with sodium pentobarbital.

PREPARATION AND INJECTION OF nNav1.5 PEPTIDE TO A POSITIVE CONTROL GROUP

In total, four injections of nNav1.5 peptide were delivered to the positive control mice in an interval of 14 days. The first injection was delivered at day 0, approximately 200  $\mu$ L of 0.25 mg/mL nNav1.5 peptide solution was mixed with 200  $\mu$ L of 100  $\mu$ g/mL alum. The solution (alum and peptide) was left in a 37 °C incubator for 30 min. Approximately 300  $\mu$ L of the solution was delivered subcutaneously. On day 14, the same dosage of nNav1.5 peptide conjugated with alum was delivered via subcutaneous injection. The third and fourth injection was delivered on day 28 and day 42, respectively, however this time, only 300  $\mu$ L of 0.25 mg/mL nNav1.5 peptide solution was delivered via intraperitoneal injection. The combination of different routes and sites of injection of peptide has been carried out as recommended by previous studies and literatures (Felio et al. 2009; Greenfield et al. 2020; Okuda et al. 2019). This procedure was shown to produce more effective immunisation and induce a stronger immune response compared to the administration of subcutaneous injection alone (Uddback et al. 2016). On day 56, all three mice were anaesthetised with sodium pentobarbital and sacrificed.

COLLECTION OF ORGANS, WHOLE BLOOD, AND SERUM

All 4T1 orthotopic and normal control mice were subjected to blood and organ collection, however, only blood collection was carried out for the positive control group. Among the organs collected were the heart, liver, lungs, kidneys, brain, and spleen. Once the heads of the mice were decapitated, the dripping blood was collected into two tubes, a 1.5 mL plain Eppendorf tube and a 2 mL tube filled with RNeasy (Qiagen). Once collected, the 1.5 mL Eppendorf tube was centrifuged at a speed of  $877 \times g$  for about 10 min at 4 °C to separate the serum from the whole blood. The whole blood collected in the

2 mL containing RNeasy was kept at 4 °C for RNA extraction on the next day. The resected tumours and organs such as the heart, liver, lungs, kidneys, brain, and spleen were examined grossly and kept in 37% formalin (Merck). Meanwhile, for the positive control group, only serum samples were collected and pooled together.

HISTOPATHOLOGICAL ANALYSIS

Standard haematoxylin and eosin staining of paraffin-embedded tissue were used for histological examination of primary tumours and metastases on the target organs. Stained sections were examined for signs of metastasis and photographed using *Olympus BX41* light microscope and *CellSensor* software, respectively. The metastatic foci in the lungs, spleen, kidney, and heart of eight 4T1 orthotopic mice were counted under 10X magnification and had been verified by a certified pathologist.

RNA EXTRACTION, CDNA CONVERSION, AND REAL-TIME PCR

The RNA extraction of the whole blood samples of the mice was performed by using the Mouse Ribopure-Blood RNA isolation kit (*Invitrogen*). The manufacturer's protocol was followed meticulously. The RNA yield was estimated by measuring the absorbance at 260 nm using *TECAN Nanoquant Infinite 200 Pro* multimode microplate reader followed by the assessment of RNA purity from the ratio of absorbance at 260 and 280 nm. Agarose gel electrophoresis was conducted to assess the RNA integrity. The extracted RNA was converted into cDNA using *High-Capacity RNA-to-cDNA™* Kit (*Applied Biosystems*). The real-time PCR analysis was conducted using *PrimeTime Mini* qPCR assay Taqman Assay (*Integrated DNA Technologies*), which detects the nNav1.5 sequence and house-keeping gene, beta-actin gene ( *$\beta$ -actin*). The sequences of the primers used are as follows (Table 1).

TABLE 1. Primer and probe sequence of nNav1.5 and  $\beta$ -actin

Genes	Primer and probe sequence
nNav1.5 (NM_021544.4)	Primer 1: 5' TGAAATCGTTTTTCAGAGCTCTC 3' Primer 2: 5' TCATGGCGTATGTATCAGAGAA 3' Probe sequence: 5'/56-FAM/CGAAGAGCC/ZEN/GACAAATTGCCTAGCTTTAT/3IABkFQ/3'
$\beta$ -actin (M.m.P.T.58.33540333)	Primer 1: 5' GCGAGCACAGCTTCTTTG 3' Primer 2: 5' ATGCCGGAGCCGTTGTC 3' Probe sequence: 5'/56-FAM/CCGCCACCA/ZEN/GTTCGCCATG/3IABkFQ/3'

Quantitative real-time was performed in *Applied Biosystem Prism 7500* real-time PCR system (*Thermo Fisher Scientific*) and the amplification conditions were as follows: Initial polymerase activation for 3 min at 95 °C for one cycle, followed by amplification (40 cycles): denaturation for 15 s at 95 °C and 1 min at 60 °C.  $C_t$  values of the nNav1.5 gene were normalised to  $\beta$ -actin (housekeeping gene) and the relative mRNA expression of target genes were calculated by the  $2^{-\Delta C_t}$  quantitative method (Schmittgen & Livak 2008), for each mouse (individual data point).

IN-HOUSE INDIRECT ENZYME-LINKED  
IMMUNOSORBENT ASSAY (ELISA): DETECTION OF  
ANTI-nNav1.5-Ab IN THE SERUM OF CONTROL AND 4T1  
ORTHOTOPIC MICE MODELS

Since there is no commercial ELISA kit available for the detection of anti-nNav1.5-Ab, an optimised in-house indirect ELISA was performed to detect the presence of antibodies produced against nNav1.5 antigen found in the serum. The 96-well ELISA plate (*Nunc Maxisorp*) was coated with 100  $\mu$ L of nNav1.5 peptide (*GenScript*) working solution (5  $\mu$ g/mL). The plate was left to rest at 4 °C overnight. After the overnight incubation, the plate was washed with PBS, three times. The non-specific sites were blocked with 200  $\mu$ L of 5% skim milk for 2 h. The previous washing step was repeated. The serum samples of 100  $\mu$ L at a dilution of 1:25 was added (for the serum samples retrieved from control and 4T1 orthotopic mice model groups). The serum samples retrieved from the positive sera group were diluted into four dilutions; 1:25, 1:50, 1:100 and 1:200 and approximately, 100  $\mu$ L of each dilution were loaded into their respective wells. The plate was left to rest at 4 °C overnight. On the third day, similar wash process was repeated with PBS-TWEEN 20, before incubating the plate with 100  $\mu$ L of secondary antibody at a dilution of 1:1000 dilution. The secondary antibody used in this study was peroxidase conjugated affinity purified goat anti-mouse IgG (H&L) (*Origene*). The plate was left to rest at 4 °C for 2 h. After the incubation, the plate was washed again with PBS-TWEEN 20, three times followed by the addition of 100  $\mu$ L of 3,3',5,5'-Tetramethylbenzidine (TMB) substrate. The substrate was left to incubate for about 30 min. Hydrochloric acid was added to stop the reaction and the absorbances were read spectrophotometrically at 450 nm. The optical density of each sample was scanned using *Thermo Scientific's Varioskan Flash Spectral Scanning Multimode Reader*.

THE QUANTIFICATION OF INTERLEUKIN-6 (IL-6) IN THE  
SERUM OF CONTROL AND 4T1 ORTHOTOPIC MICE

The IL-6 sandwich ELISA assay kit (E-EL-M0044) was purchased from *Elabscience*. The standards were prepared as instructed by the manufacturer. The serum samples were diluted in the sample diluent (provided in the kit) in the ratio of 1:16. Once diluted, 100  $\mu$ L of diluted serum and standard solution were loaded into their respective wells followed by incubation at 37 °C for 90 min. The wells were then emptied and 100  $\mu$ L of biotinylated detection solution was added into each well immediately. The incubation of the biotinylated detection solution took place at 37 °C for 1 h. After the incubation period had ended, the wells were washed with 350  $\mu$ L of wash buffer about three times. Next, 100  $\mu$ L of horseradish peroxidase substrate conjugated solution was added into each well and the incubation took about 30 min at 37 °C. The previous washing step was repeated five times. Once washed, 90  $\mu$ L of substrate solution was added into each well and was allowed to incubate at 37 °C for 30 min before the addition of 50  $\mu$ L of stop solution. The absorbances were read at a wavelength of 450 nm using *Thermo Scientific's Varioskan Flash Spectral Scanning Multimode Reader*.

THE QUANTIFICATION OF VASCULAR ENDOTHELIAL  
GROWTH FACTOR (VEGF) IN THE SERUM OF CONTROL  
AND 4T1 ORTHOTOPIC MICE MODELS

Mouse VEGF *Quantikine* ELISA Kit, MMV00 (*R&D systems*), was used for the quantification of VEGF in the mice serum. The serum samples were diluted (with the provided sample diluent) in the ratio of 1:4. The other reagents were prepared according to the given protocol. Approximately, 50  $\mu$ L of assay diluent RD1N was added into each well, followed by the addition of standards and diluted samples. The added solutions were mixed gently using a shaker and left to incubate at room temperature for 2 h. After 2 h, the solutions were decanted, followed by washing of the wells five times using 400  $\mu$ L of wash buffer prepared earlier. Approximately, 100  $\mu$ L of mouse VEGF conjugate was added into each well and incubated at room temperature for 2 h. After 2 h, the washing step was repeated. Once washed, 100  $\mu$ L of substrate solution was added to each well and incubated at room temperature for 30 min. Stop solution (100  $\mu$ L) was finally added and the absorbances were determined at 540 nm using *Thermo Scientific's Varioskan Flash Spectral Scanning Multimode Reader*.

STUDY II: A CLINICAL STUDY USING SERUM SAMPLES  
FROM BCA PATIENTS  
SAMPLE SIZE, LOCATION OF STUDY, AND ETHICAL  
APPROVAL

A sample size of 32 BCa patients (mean age  $\pm$  SD =  $49.16 \pm 12.69$ ) was recruited after obtaining their written informed consents. The recruitment of the patients was conducted at the Hospital Universiti Sains Malaysia (HUSM) in collaboration with the USM Breast Cancer Awareness and Research Unit (BestARi) (Kubang Kerian, Malaysia). The ethical approval was granted by the Human Research Ethics Committee of USM (JEPeM) (approval no. USM/JEPeM/18100518).

INCLUSION AND EXCLUSION CRITERIA OF BCA  
PATIENTS

The selected BCa patients were diagnosed with either an early-invasive (stage I and stage II) or advanced (stage III and IV) stage of BCa, based on the TNM guidelines (Giuliano et al. 2018). Other criteria included were: (ii) no past history of other types of cancer, (iii) have not received any treatments, and (iv) do not have any chronic diseases such as immune disorders, chronic diabetes, and hypertension. BCa patients who do not satisfy these requirements were excluded from the study.

COLLECTION OF BLOOD SAMPLES

Approximately 3 mL of whole blood was withdrawn from each BCa patient. The clot-activator tube containing the blood sample was centrifuged for at least 15 min at  $1800 \times g$  to separate the serum. The serum samples were stored at  $-80^\circ\text{C}$ .

IN-HOUSE INDIRECT ENZYME-LINKED  
IMMUNOSORBENT ASSAY (ELISA): DETECTION OF ANTI-  
nNav1.5-Ab IN THE SERUM OF BCA PATIENTS

The procedure has been adapted from our previous publication (Rajaratnam et al. 2021). The protocol of the human indirect ELISA is quite similar to those applied in the animal study. There were several changes made such as the dilution factor for the serum samples (1:400) and the secondary antibody (1:5000). The secondary antibody used was H+L rabbit anti-human IgG, HRP conjugated secondary antibody (*Cusabio Technology*).

STATISTICAL ANALYSIS

The normality of the statistical data sets was determined and followed by the inspection of the skewness and kurtosis (Mishra et al. 2019). Data sets that met the

required normality criteria were subjected to parametric analysis such as Student T-test and those which did not, was subjected to non-parametric analysis such as the Mann-Whitney U test. The error bars in the figure graphs either represent standard deviation (for Student T-test) and interquartile range (for Mann Whitney-U test). Spearman correlation was conducted as well. The evaluation of r-value was conducted based on the guidelines provided by (Norsa`adah 2013).  $P \leq 0.05$  was considered to indicate a statistically significant difference.

RESULTS

STUDY I: PRECLINICAL ANIMAL STUDY USING 4T1  
ORTHOTOPIC BCA MICE MODEL

The pattern of 4T1 tumour development and signs of metastasis on the target organs in the 4T1 orthotopic mice model were assessed followed by the detection of circulating nNav1.5 in the blood and anti-nNav1.5-Ab in the serum of 4T1 orthotopic mice.

DEVELOPMENT OF 4T1 ORTHOTOPIC MICE MODELS

The duration of 4T1 orthotopic mice model development was 42 days (6 weeks) (Figure 1(a) & 1(b)). All 17 mice developed a 4T1 tumour. Regression in the volume of the 4T1 tumour was detected in week 5 of its development as illustrated in Figure 1(c). None of the 40 mice died before the end of the experimental period indicating 100% survival despite the worsening of the overall health among the 4T1 tumour-bearing mice.

HISTOPATHOLOGICAL ANALYSIS ON THE CROSS-  
SECTION OF 4T1 TUMOUR AND TARGET ORGANS

Gross examination showed prominent abnormalities in the lungs, liver, spleen, and heart of 4T1 orthotopic mice (Supplementary Table 1). The staining of the 4T1 tumour showed the presence of a mix of hyperchromatic and vesicular nuclei as well as eosinophilic and scanty cytoplasm. A large area of necrosis was observed at the centre of the cross-section (Figure 2). Intratumoral vessels were also observed as portrayed in Figure 2. There were signs of BCa metastasis on the heart, lungs, spleen, liver, and kidneys seen in the organs retrieved from the 4T1 orthotopic mice group which were not observed in those of control mice (Figure 3). There was no metastasis detected in any parts of the brain resected from the 4T1 orthotopic mice. Vessel invasions were seen in the heart, lungs, liver, kidneys, and spleen but none were observed in the brain (not shown).

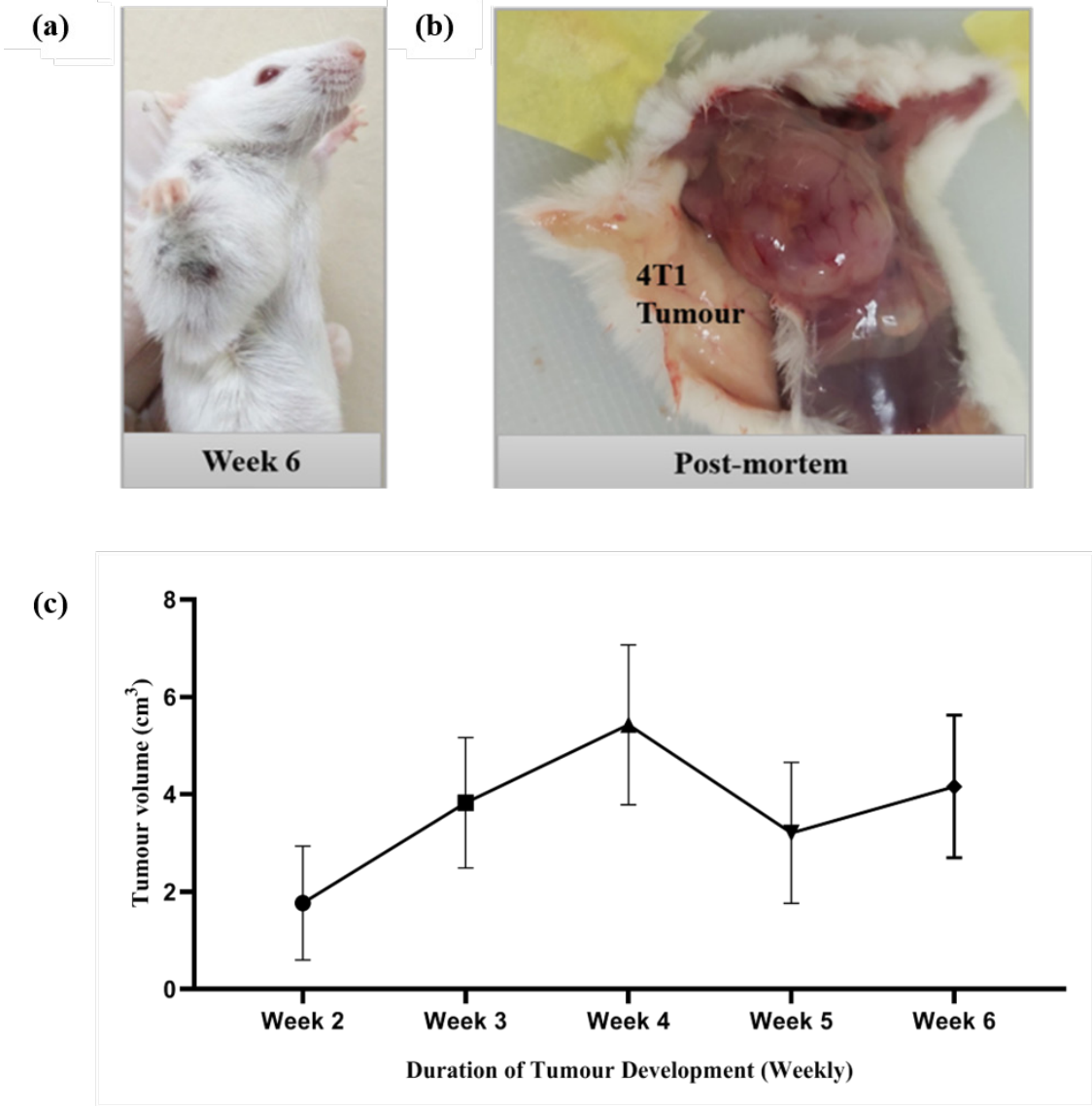


FIGURE 1. The development of the 4T1 breast tumour towards the end of six weeks. (a) The tumour growth recorded in week 6, where the necrotic spot can be observed, (b) The post-mortem of the 4T1 orthotopic mice, where the tumour appears to be intensively vascularised, and (c) The pattern of tumour development throughout a period of 6 weeks (42 days). The error bars represent the standard deviation

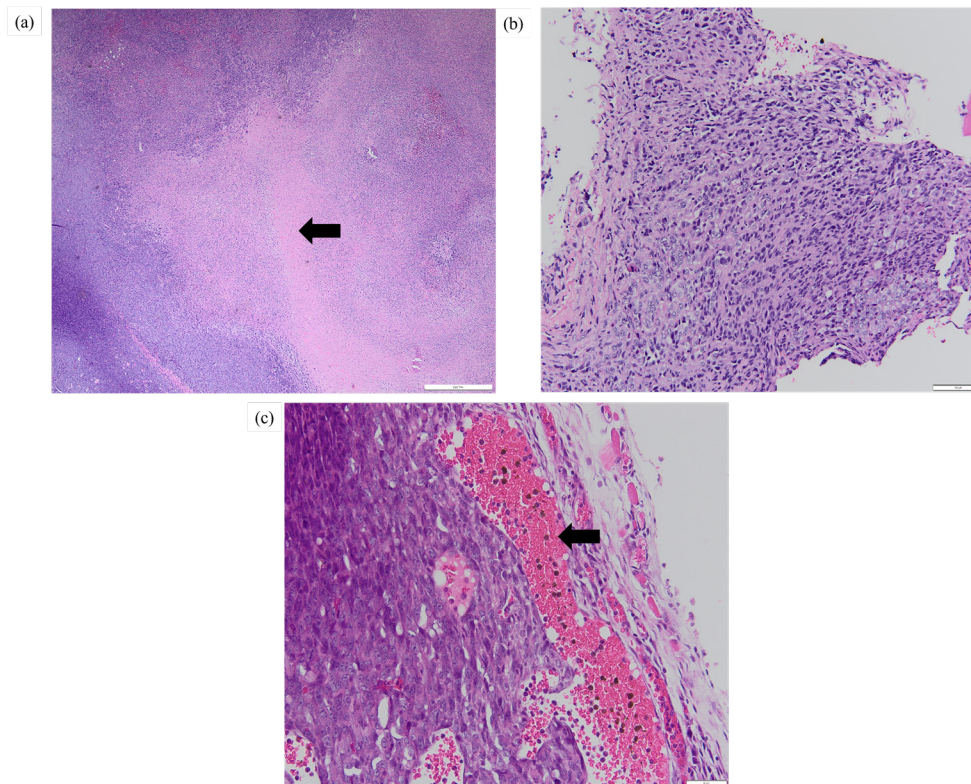


FIGURE 2. Histology of 4T1 tumour. (a) The presence of necrosis was observed at the center of the primary tumour (marked by the black arrow) under 4× magnification, (b) Spindle-shaped nuclei were observed at some parts of the primary tumour under 20× magnification, and (c) The presence of blood vessels (marked by the black arrow) within the primary tumour was observed under 20× magnification

#### THE DETECTION OF nNav1.5 ANTIGEN IN THE BLOOD SAMPLES OF 4T1 ORTHOTOPIC MICE

There were presences of nNav1.5 antigen in the blood samples retrieved from the 4T1 orthotopic mice group. The  $2^{-\Delta Ct}$  values ranged from  $3.4573 \times 10^{-5}$  to 0.3015. However, the expression of nNav1.5 was completely absent (no amplification) in the control mice (similarly to the non-template control) which confirmed the absence of anti-nNav1.5-Ab in the serum of the control mice.

#### ANTI-nNav1.5-AB EXPRESSION IN THE SERUM OF 4T1 ORTHOTOPIC MICE MODELS

The positive control sera were used to test the indirect ELISA assembly. However, the standard curve (Supplementary Figure 1) could not be used as a template to interpolate the concentration of anti-nNav1.5-Ab as the methods of induction of nNav1.5 antigen were different in both models. The absorbance values of anti-nNav1.5-Ab were significantly higher from the wells

that were incubated with the serum of 4T1 orthotopic mice model compared to those of the control mice ( $P < 0.0001^{***}$ ) (Figure 4(a)). Based on the receiver operating characteristic curve (ROC) analysis made, the sensitivity and specificity of the assay were both 100% and the cut-off value of the assay was  $>2.759$ . Absorbance above the cut-off value was deemed as positive for the presence of anti-nNav1.5-Ab. Based on the cut-off value, none of the serum samples collected from control mice exhibited a positive presence of anti-nNav1.5-Ab (Supplementary Table 2). In contrast, all the 4T1 mice exhibited a positive presence of anti-nNav1.5-Ab with absorbance higher than the cut-off value (Supplementary Table 2). Spearman correlation analysis (Figure 4(b)) which was conducted between the expression of nNav1.5 antigens and anti-nNav1.5-Ab in the serum showed that there was a significant-good negative correlation ( $P$ -value=0.0245\*,  $r$ -value=-0.5486).

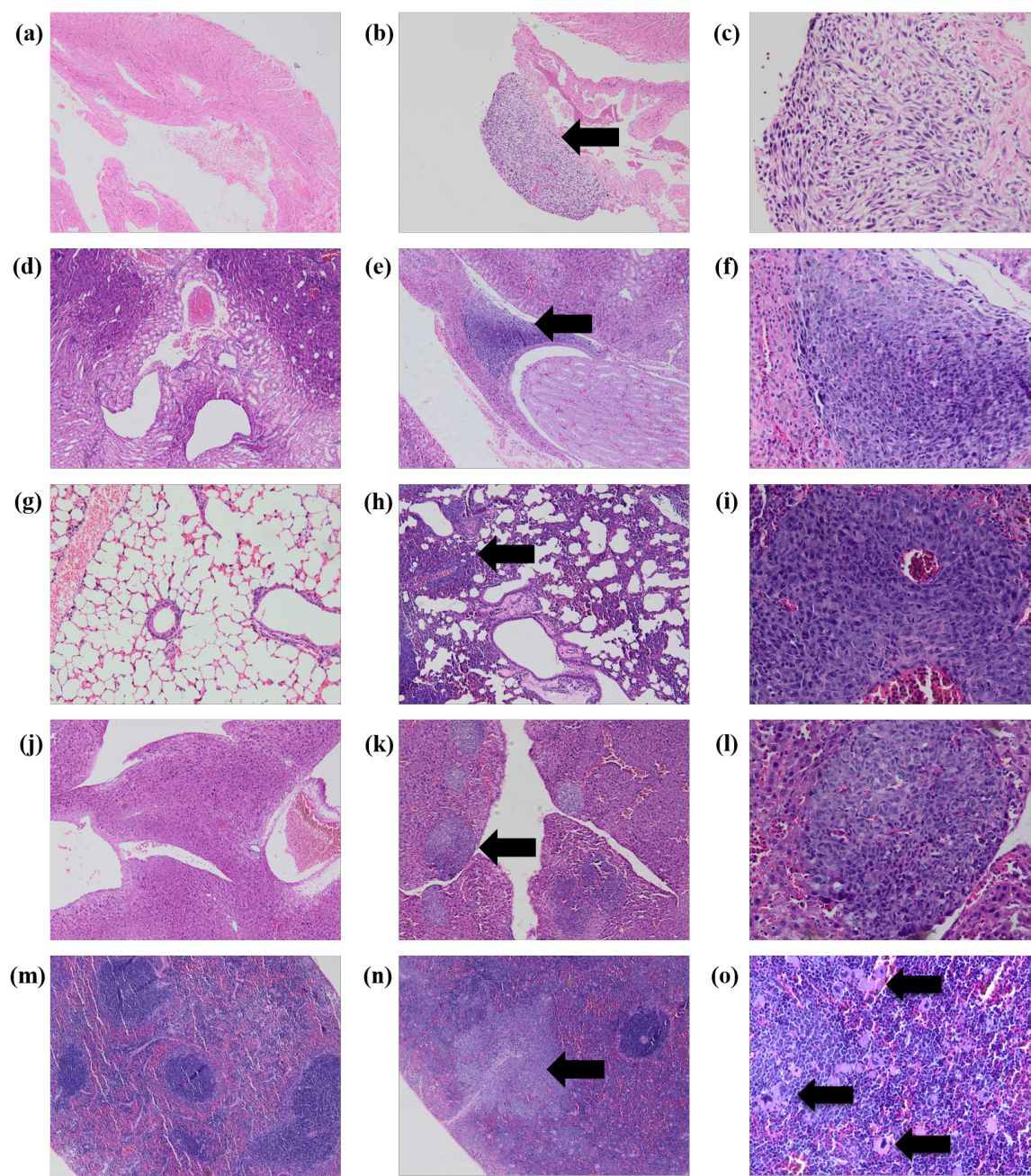


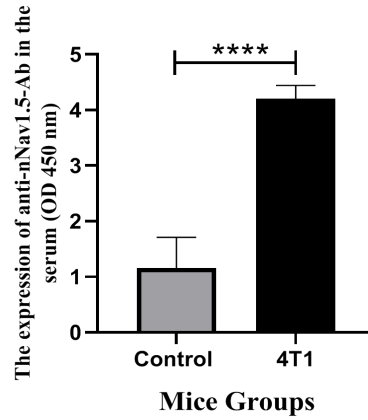
**FIGURE 3.** Histology of the target organs retrieved from 4T1 orthotopic and control mice. (a) Signs of metastasis were not detected in the heart resected from control mice at 10× magnification, (b) The presence of metastasis on the heart (highlighted by the arrow), resected from the 4T1 mice at 10X magnification, (c) The presence of spindle-shaped cancer cells was seen at the heart of 4T1 mice, similar to those of the primary tumour at 40× magnification, (d) Signs of metastasis were not detected in the kidney resected from control mice at 10× magnification, (e) The presence of invasion of metastatic cells at the kidney (highlighted by the arrow), resected from the 4T1 mice at 10× magnification, (f) Under 40× magnification, the tumour cells exhibited a mixed presence of hyperchromatic and vesicular nuclei (pleomorphic) as well as eosinophilic cytoplasm observed, (g) There was an absence of any signs of metastasis in the lungs resected from control mice under 10× magnification. The alveolar walls were one-cell thick, (h) Lung tissue-section showed infiltration by malignant tumour cells that appear in clusters (highlighted by the arrow). The alveolar walls were infiltrated with tumours cells causing the alveolar space to reduce in size. There were marked disturbance of lung architecture with abnormal thick-walled and collapsed alveoli (10× magnification), (i) Cytological features exhibited moderate polymorphic irregular nuclei (a mixture of hyperchromatic and vesicular nuclei) under 40× magnification, (j) There was an absence of any signs of metastasis in the liver resected from control mice under 10× magnification, (k) Clusters of tumour cells (highlighted by the arrow) seen in the liver sections retrieved from 4T1 mice group under 10× magnification, (l) These clusters were prominent at the edges of the lobes along with the endothelial cells of the blood vessels. The clusters consisted of tumour cells with a mix of hyperchromatic and vesicular nuclei under 40× magnification, (m) There was an absence of any signs of metastasis in the spleen resected from control mice under 10× magnification, (n) There was an invasion of tumour cells within the spleen retrieved from the 4T1 mice, portrayed as a ‘foggy’ cluster (highlighted by the arrow) under 10× magnification, and (o) Giant tumour cells (marked by black arrows) were observed under 40× magnification

THE CORRELATION BETWEEN THE TOTAL OF  
METASTATIC FOCI AND THE EXPRESSION OF ANTI-  
nNav1.5-Ab

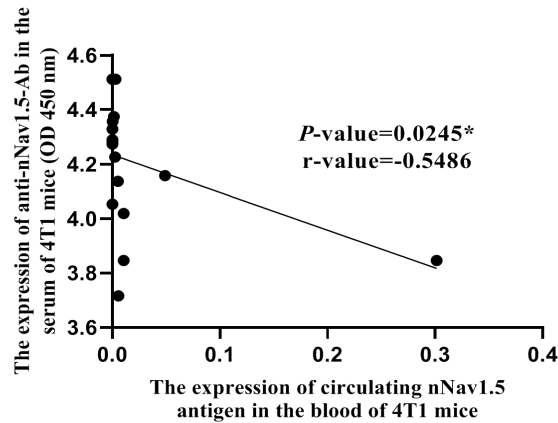
There was a significant negative correlation ( $P=0.0485^*$ ,

$r=-0.7306$ ) between the total metastatic foci (in the lungs, spleen, kidney, and heart) and the expression of anti-nNav1.5-Ab (Figure 4(c)).

(a)



(b)



(c)

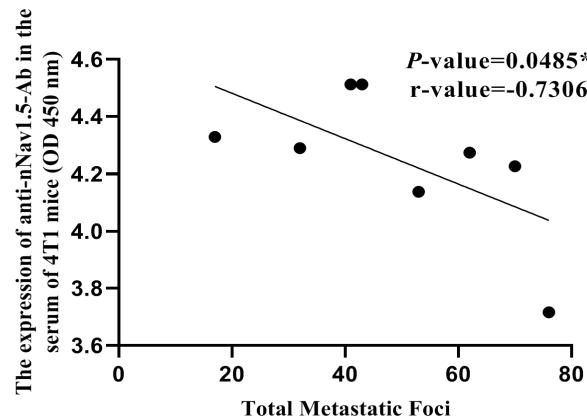


FIGURE 4. The comparison in the expression of anti-nNav1.5-Ab in the serum of 4T1 orthotopic and control mice. (a) The difference in the expression of anti-nNav1.5-Ab in the serum samples of control ( $n=20$ ) and 4T1 orthotopic mice ( $n=17$ ) was analysed using Student T-test, (b) The correlation between expression of nNav1.5 antigen and anti-nNav1.5-Ab in the serum of 4T1 orthotopic mice models ( $n=17$ ). Note: \*indicates  $P\leq 0.05$ , and (c) The correlation between the expression of anti-nNav1.5-Ab and the total metastatic foci of 4T1 tumour ( $n=8$ )

QUANTIFICATION OF IL-6 AND VEGF IN THE SERUM OF  
4T1 ORTHOTOPIC MICE MODEL

The standard curve was plotted based on the corrected absorbance values for each standard concentration, in both analyses of IL-6 and VEGF (Supplementary Figure 2). The serum collected from 4T1 orthotopic mice models exhibited a higher concentration of IL-6 compared to those of control mice. However, the difference was not statistically significant ( $P=0.1650$ ) (Figure 5(a)). Based on the Spearman correlation analysis conducted,

there was a significant positive correlation between the expression of anti-nNav1.5-Ab and the concentration of IL-6 in the serum of 4T1 orthotopic mice model (Figure 5(b)). In the VEGF analysis, the serum collected from 4T1 orthotopic mice models exhibited a significantly higher concentration of VEGF compared to those of control mice ( $P<0.0001$ \*\*\*\*) (Figure 5(c)). Similarly, VEGF also portrayed a significant positive correlation with the expression of anti-nNav1.5-Ab in the serum of 4T1 mice (Figure 5(d)).

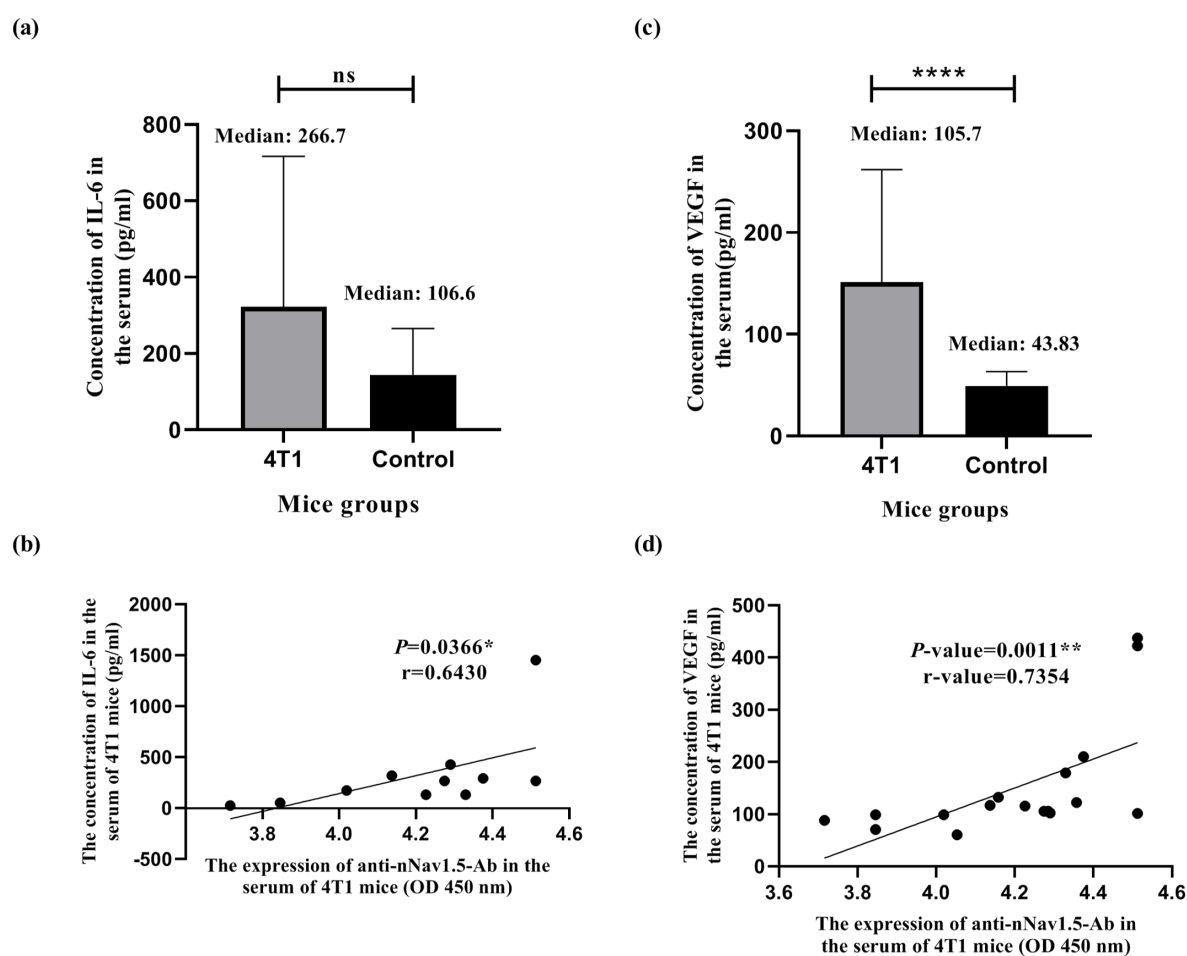


FIGURE 5. The quantification of cytokines in serum of 4T1 orthotopic and control mice and the correlation between the concentration of cytokines and the expression of anti-nNav1.5-Ab. (a) The difference in the concentration of IL-6 in the serum of 4T1 orthotopic ( $n=11$ ) and control mice ( $n=11$ ), analysed using Mann-Whitney test, (b) The correlation between the concentration of IL-6 and expression of anti-nNav1.5-Ab in the serum of 4T1 orthotopic mice ( $n=11$  pairs), (c) The difference in the concentration of VEGF in the serum of 4T1 orthotopic ( $n=17$ ) and control mice ( $n=20$ ), analysed using Mann-Whitney test, and (d) The correlation between the concentration of VEGF and expression of anti-nNav1.5-Ab in the serum of 4T1 orthotopic mice ( $n=17$  pairs). Note: ns indicates non-significant  $P$ -value, \* indicates  $P\leq 0.05$ , \*\* indicates  $P\leq 0.01$  & \*\*\*\* indicates  $P\leq 0.0001$

STUDY II: A CLINICAL STUDY USING SERUM SAMPLES FROM BCa PATIENTS ANTI-nNav1.5-AB EXPRESSION IN THE SERUM OF BCa PATIENTS

The patients who are diagnosed with advanced-stages

of BCa exhibited significantly higher expression of anti-nNav1.5-Ab in comparison with those diagnosed with early-invasive BCa stages ( $P=0.0110^*$ ) (Figure 6).

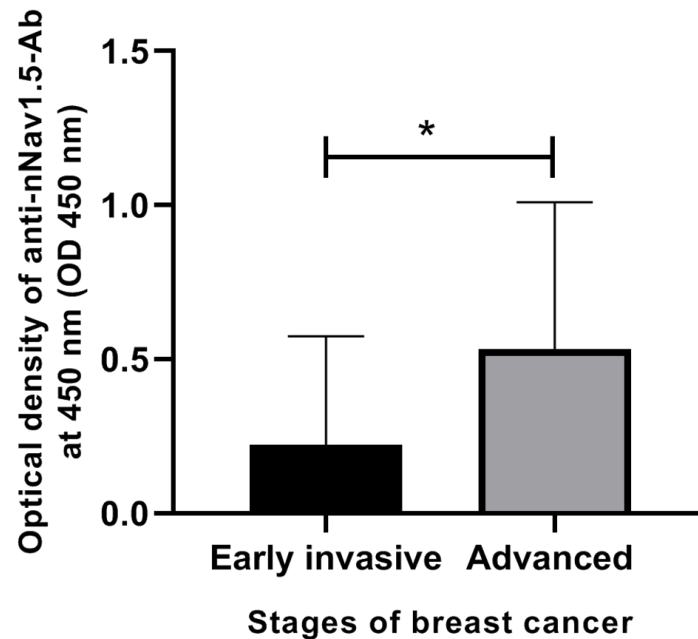


FIGURE 6. The comparison in the absorbances of anti-nNav1.5-Ab in the early-invasive and advanced BCs stages. Patients who are diagnosed with advanced-stages of BCa portrayed higher expression of anti-nNav1.5-Ab compared to those diagnosed with early-invasive stages of BCa ( $P=0.0110^*$ ). Note: \*indicates  $P \leq 0.05$

## DISCUSSION

### STUDY I: PRECLINICAL ANIMAL STUDY USING 4T1 ORTHOTOPIC BCa MICE MODEL

Metastasis is a multifaceted process that is entwined with several other processes, including angiogenesis (Madu et al. 2020), invasion (Stuelten et al. 2018), and immune evasion (Jones et al. 2018). Increased expression of nNav1.5 has been reported to exacerbate the metastatic capacity of BCa cells (Brackenbury et al. 2007; Fraser et al. 2005). The purpose of this preclinical animal study was to determine the presence of circulating nNav1.5 antigen and anti-nNav1.5-Ab in accordance with BCa metastasis. The preclinical study was conducted by inoculating 4T1 cells orthotopically into *in vivo* mouse model to mimic the late stage of human BCa.

Before examining the presence of nNav1.5 and anti-nNav1.5-Ab in association with BCa metastasis, it is necessary to establish the disease context. Histology and cytokine analyses were used to validate the presence of metastasis in the 4T1 orthotopic mice model. In contrast, such a condition was absent in control mice. In the current study, two cytokines were analysed to depict the condition of the metastatic microenvironment within the 4T1 mice model compared to control mice. The upregulation of IL-6 supports the progression and survival of metastatic BCa cells (Chang et al. 2013; Masjedi et al. 2018). In favour of tumour progression, IL-6 also facilitates angiogenesis by upregulating VEGF production (Chang et al. 2013; Kujawski et al. 2008; Masjedi et al. 2018). Angiogenesis is an important factor that sustains the progression of metastatic BCa (Adams et al. 2000). 4T1 tumour is a

highly vascularised mammary cancer, whereby large blood vessels were observed during a gross examination and via histology. In short, the upregulated level of IL-6 and VEGF in 4T1 orthotopic mice validates the metastatic microenvironment.

After confirming the presence of metastasis in the animal model, circulating nNav1.5 antigen was investigated. We were able to report the presence of circulating nNav1.5 antigen in blood samples for the first time, rather than extracting it from the 4T1 primary tumour. As expected, there was no detectable circulating nNav1.5 antigen in the blood of control mice. Yamaci et al. (2017) previously demonstrated the presence of nNav1.5 in normal healthy breast epithelial tissue. In clinical practice, such interpretations based on tissue samples may result in the presence of false-positive results. Due to the absence of circulating nNav1.5 in control mice, using blood samples may prevent the false detection of nNav1.5 that could be misinterpreted as early signs of BCa.

Detecting circulating nNav1.5 antigen is similar to performing a liquid biopsy. Liquid biopsy is a novel diagnostic concept that utilises non-solid biological tissues such as blood. Liquid biopsy is less invasive than tissue-based biopsy. The common cornerstones of liquid biopsy are circulating tumour cells (CTCs) and circulating tumour DNA (Ye et al. 2019). However, in this study, the detection of nNav1.5 was conducted using RNA extracted from the blood samples. The cellular response or functional role of VGSCs may be manipulated to serve a specific purpose. These changes can be carried out at two main levels, which are transcriptional and translation. According to Diss et al. (2004), the mechanism of producing alternative-splice is classified under transcriptional modification. Since transcription mainly involves RNA as the main nucleic acid, it is more appropriate to extract RNA instead of DNA, to study the expression of circulating nNav1.5. The RNA-based detection of circulating nNav1.5 is less tedious than evaluating nNav1.5 using CTCs, as it does not involve the isolation of CTCs. Another disadvantage of using CTCs is that the limited number of CTCs shed into the circulation by the primary tumour, which may be insufficient (Potdar & Lotey 2015) to justify the expression of nNav1.5.

The biphasic growth pattern in the 4T1 tumour volume may be associated with the production of antibodies against 4T1 antigens, cytokines, and the presence of myeloid-derived suppressor cells (MDSCs) (Tao et al. 2008). In addition, the upregulation of

IL-6 may have also contributed to the relapse in the tumour volume at the end of 4T1 tumour development. According to Tsukamoto et al. (2018), IL-6 can dampen the immune system by directing the myeloid cells to produce immunosuppressive molecules, which cause the generation of antigen tolerant M2 macrophages.

As anticipated, the expression of anti-nNav1.5-Ab was only positively detected above the cut-off value in the serum of 4T1 orthotopic BCa mice models. These novel antibodies were only reported in all 17 tumour-bearing mice, which portrayed the presence of BCa metastasis. The significant negative correlation between the expressions of nNav1.5 and anti-nNav1.5-Ab may imply the attempt of the immune system to eradicate the presence of nNav1.5 antigen and retard the progression of BCa metastasis. The inverse relationship between nNav1.5 antigen and its antibody opens a new perspective on the immunotherapeutic prospect of anti-nNav1.5-Ab in treating BCa metastasis. An *in vivo* study by Gao et al. (2019) highlighted the use of an antibody known as Nav1.5-third extracellular region antibody (E3Ab) to downregulate the volume of ovarian tumour. Therefore, it is reasonable to consider that anti-nNav1.5-Ab may possess the immunotherapeutic potential to neutralise the expression of nNav1.5.

In this study, total metastatic foci accumulated from the lungs, spleen, kidney and heart of 4T1 mice were counted. The metastatic foci in the liver were not counted because they exhibited replacement and sinusoidal growth patterns which make it difficult to clearly distinguish the tumour border. The inverse relationship between the total number of metastatic foci and the expression of anti-nNav1.5-Ab may indicate the role of these novel antibodies in retarding the progression of metastasis. This further solidifies the connection between anti-nNav1.5-Ab and BCa metastasis. Higher expression of anti-nNav1.5-Ab reflects a lower expression of nNav1.5 antigen and slowed progression of metastasis.

Furthermore, the significant positive correlations between the expression of anti-nNav1.5-Ab and the pro-inflammatory cytokines, IL-6 and VEGF, signify the capacity of anti-nNav1.5-Ab as a novel metastasis marker to detect the presence of BCa metastasis. Moreover, VGSCs (particularly Nav1.5) have been reported to exhibit angiogenic function in modulating the VEGF-induced ERK activation via the PKC $\alpha$ -B-RAF signalling axis (Andrikopoulos et al. 2011). This statement could also explain the positive correlation between the upsurge of VEGF and anti-nNav1.5-Ab (as it reflects the presence of nNav1.5).

STUDY II: A CLINICAL STUDY USING SERUM SAMPLES  
FROM BCA PATIENTS

The findings obtained from the animal study, especially on anti-nNav1.5-Ab were solidified with the incorporation of a clinical study using serum samples from BCA patients. Anti-nNav1.5-Ab expression was significantly increased in the serum of BCA patients with advanced-stage, indicating that the presence of BCA metastasis influences the expression of anti-nNav1.5-Ab. According to the TNM staging system, metastasis is more likely to occur in advanced human BCA, particularly stage IV (Giuliano et al. 2018). As expected, the high expression of anti-nNav1.5-Ab reflects the prominent lymph node and metastasis involvement in advanced stages of BCA (stage III and IV). This is also in agreement with the findings reported by Fraser et al. (2005), which emphasised on the correlation between nNav1.5 and lymph node metastasis.

CONCLUSIONS

In a nutshell, the detection of nNav1.5 antigen and anti-nNav1.5-Ab is consistent with the presence of metastasis, from the perspective of both preclinical and clinical studies. The detection of circulating nNav1.5 antigen and anti-nNav1.5-Ab in blood, suggests a less invasive approach as compared to the utilisation of BCA tissues. As for the limitation of the study, the absence of comparative results using conventional markers such as CA15-3 and other established cytokines should have been implemented as this could have highlighted the potential of nNav1.5 and anti-nNav1.5-Ab as metastatic markers to detect the progression of BCA.

ACKNOWLEDGEMENTS

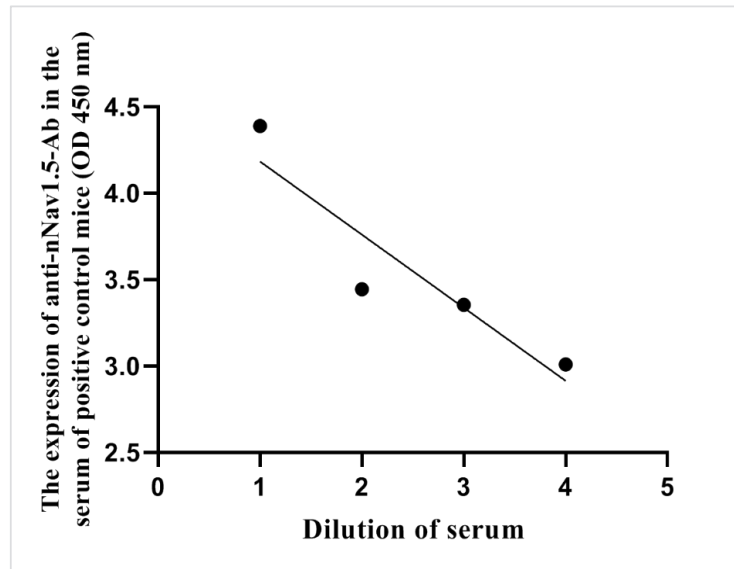
This research was funded by Universiti Sains Malaysia Research University Individual (RUI) grant (grant holder: Wan Ezumi Mohd Fuad, grant number 1001/PPSK/8012275).

REFERENCES

- Adams, J., Carder, P.J., Downey, S., Forbes, M.A., MacLennan, K., Allgar, V., Kaufman, S., Hallam, S., Bicknell, R., Walker, J.J., Cairnduff, F., Selby, P.J., Perren, T.J., Lansdown, M. & Banks, R.E. 2000. Vascular endothelial growth factor (VEGF) in breast cancer: Comparison of plasma, serum, and tissue VEGF and microvessel density and effects of tamoxifen. *Cancer Research* 60(11): 2898-2905.
- Andrikopoulos, P., Fraser, S.P., Patterson, L., Ahmad, Z., Burcu, H., Ottaviani, D., Diss, J.K., Box, C., Eccles, S.A. & Djamgoz, M.B. 2011. Angiogenic functions of voltage-gated Na<sup>+</sup> Channels in human endothelial cells: Modulation of vascular endothelial growth factor (VEGF) signaling. *Journal of Biological Chemistry* 286: 16846-16860.
- Brackenbury, W.J., Chioni, A.M., Diss, J.K.J. & Djamgoz, M.B.A. 2007. The neonatal splice variant of Nav1.5 potentiates *in vitro* invasive behavior of MDA-MB-231 human breast cancer cells. *Breast Cancer Research and Treatment* 101: 149-160.
- Brackenbury, W.J. 2012. Voltage-gated sodium channels and metastatic disease. *Channels (Austin)* 6: 352-361.
- Catterall, W.A. 2000. From ionic currents to molecular mechanisms: The structure and function of voltage-gated sodium channels. *Neuron* 26: 13-25.
- Chang, Q., Bournazou, E., Sansone, P., Berishaj, M., Gao, S.P., Daly, L., Wels, J., Theilen, T., Granitto, S., Zhang, X., Cotari, J., Alpaugh, M.L., de Stanchina, E., Manova, K., Li, M., Bonafe, M., Ceccarelli, C., Taffurelli, M., Santini, D., Altan-Bonnet, G., Kaplan, R., Norton, L., Nishimoto, N., Huszar, D., Layden, D. & Bromberg, J. 2013. The IL-6/JAK/Stat3 feed-forward loop drives tumorigenesis and metastasis. *Neoplasia* 15: 848-862.
- Chioni, A.M., Fraser, S.P., Pani, F., Foran, P., Wilkin, G.P., Diss, J.K. & Djamgoz, M.B. 2005. A novel polyclonal antibody specific for the Na(v)1.5 voltage-gated Na<sup>+</sup> channel 'neonatal' splice form. *Journal of Neuroscience Methods* 147: 88-98.
- Diaz, D., Delgadillo, D.M., Hernández-Gallegos, E., Ramírez-Domínguez, M.E., Hinojosa, L.M., Ortiz, C.S., Berumen, J., Camacho, J. & Gomora, J.C. 2007. Functional expression of voltage-gated sodium channels in primary cultures of human cervical cancer. *Journal Cell Physiology* 210: 469-478.
- Diss, J.K., Fraser, S.P. & Djamgoz, M.B. 2004. Voltage-gated Na<sup>+</sup> channels: Multiplicity of expression, plasticity, functional implications and pathophysiological aspects. *Europe Biophysic Journal* 33: 180-193.
- Felio, K., Nguyen, H., Dascher, C.C., Choi, H.J., Li, S., Zimmer, M.I., Colmone, A., Moody, D.B., Brenner, M.B. & Wang, C.R. 2009. CD1-restricted adaptive immune responses to Mycobacteria in human group 1 CD1 transgenic mice. *The Journal of Experimental Medicine* 206: 2497-2509.
- Fraser, S.P., Diss, J.K., Chioni, A.M., Mycielska, M.E., Pan, H., Yamaci, R.F., Pani, F., Siwy, Z., Krasowska, M., Grzywna, Z., Brackenbury, W.J., Theodorou, D., Koyutürk, M., Kaya, H., Battaloglu, E., De Bella, M.T., Slade, M.J., Tolhurst, R., Palmieri, C., Jiang, J., Latchman D.S., Coombes, R.C. & Djamgoz, M.B. 2005. Voltage-gated sodium channel expression and potentiation of human breast cancer metastasis. *Clinical Cancer Research* 11: 5381-5389.
- Gao, R., Shen, Y., Cai, J., Lei, M. & Wang, Z. 2010. Expression of voltage-gated sodium channel subunit in human ovarian cancer. *Oncology Reports* 23: 1293-1299.
- Gao, R., Cao, T., Chen, H., Cai, J., Lei, M. & Wang, Z. 2019. Nav1.5-E3 antibody inhibits cancer progression. *Translational Cancer Research* 8: 44-50.
- Gillet, L., Roger, S., Besson, P., Lecaille, F., Gore, J., Bougnoux, P., Lalmanach, G. & Le Guennec, J.Y. 2009. Voltage-gated sodium channel activity promotes cysteine cathepsin-dependent invasiveness and colony growth of human cancer cells. *The Journal of Biological Chemistry* 284: 8680-8691.

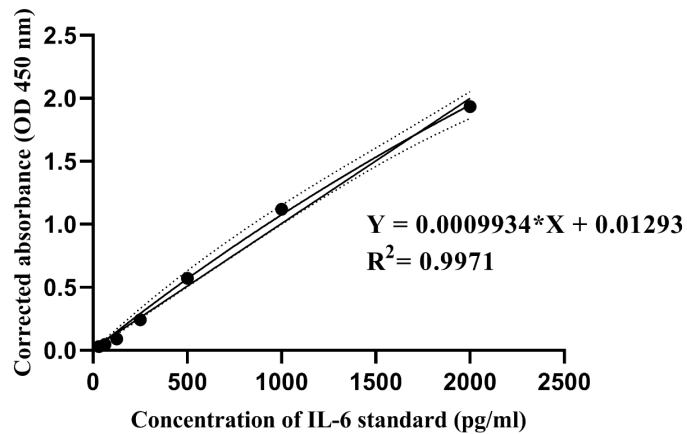
- Giuliano, A.E., Edge, S.B. & Hortobagyi, G.N. 2018. Eighth edition of the AJCC cancer staging manual: Breast cancer. *Annals of Surgical Oncology* 25: 1783-1785.
- Greenfield, E.A. 2020. Standard immunization of mice, rats, and hamsters. *Cold Spring Harbour Protocol* doi:10.1101/pdb.prot100297
- Jones, D., Pereira, E.R. & Padera, T.P. 2018. Growth and immune evasion of lymph node metastasis. *Frontiers in Oncology* 8: 36.
- Kamarulzaman, N.S., Dewadas, H.D., Leow, C.Y., Yaacob, N.S. & Mokhtar, N.F. 2017. The role of REST and HDAC2 in epigenetic dysregulation of Nav1.5 and nNav1.5 expression in breast cancer. *Cancer Cell International* 17: 74.
- Kujawski, M., Kortylewski, M., Lee, H., Herrmann, A., Kay, H. & Yu, H. 2008. Stat3 mediates myeloid cell-dependent tumor angiogenesis in mice. *The Journal of Clinical Investigation* 118(10): 3367-3377.
- Luo, Q., Wu, T., Wu, W., Chen, G., Luo, X., Jiang, L., Tao, H., Rong, M., Kang, S. & Deng, M. 2020. The functional role of voltage-gated sodium channel Nav1.5 in metastatic breast cancer. *Frontiers in Pharmacology* 11: 1111.
- Madu, C.O., Wang, S., Madu, C.O. & Lu, Y. 2020. Angiogenesis in breast cancer progression, diagnosis, and treatment. *Journal of Cancer* 11(15): 4474-4494.
- Masjedi, A., Hashemi, V., Hojjat-Farsangi, M., Ghalamfarsa, G., Azizi, G., Yousefi, M. & Jadidi-Niaragh, F. 2018. The significant role of interleukin-6 and its signaling pathway in the immunopathogenesis and treatment of breast cancer. *Biomedicine & Pharmacotherapy* 108: 1415-1424.
- Mishra, P., Pandey, C.M., Singh, U., Gupta, A., Sahu, C. & Keshri, A. 2019. Descriptive statistics and normality tests for statistical data. *Annals of Cardiac Anaesthesia* 22(1): 67-72.
- Nelson, M., Yang, M., Millican-Slater, R. & Brackenbury, W.J. 2015. Nav1.5 regulates breast tumor growth and metastatic dissemination *in vivo*. *Oncotarget* 6(32): 32914-32929.
- Norsa'adah, B. 2013. *Univariable Analyses using IBM SPSS Statistics Version 20.0*. Kota Bharu, Malaysia: Universiti Sains Malaysia.
- Okuda, T., Shimizu, K., Hasaba, S. & Date, M. 2019. Induction of specific adaptive immune responses by immunization with newly designed artificial glycosphingolipids. *Scientific Reports* 9: 18803.
- Onganer, P.U. & Djamgoz, M.B. 2005. Small-cell lung cancer (human): Potentiation of endocytic membrane activity by voltage-gated Na<sup>(+)</sup> channel expression *in vitro*. *The Journal of Membrane Biology* 204(2): 67-75.
- Onkal, R., Mattis, J.H., Fraser, S.P., Diss, J.K., Shao, D., Okuse, K. & Djamgoz, M.B. 2008. Alternative splicing of Nav1.5: An electrophysiological comparison of 'neonatal' and 'adult' isoforms and critical involvement of a lysine residue. *Journal of Cellular Physiology* 216(3): 716-726.
- Paschall, A.V. & Liu, K. 2016. An orthotopic mouse model of spontaneous breast cancer metastasis. *Journal of Visualized Experiments* 114: 54040.
- Patel, F. & Brackenbury, W.J. 2015. Dual roles of voltage-gated sodium channels in development and cancer. *The International Journal of Developmental Biology* 59(7-9): 357-366.
- Potdar, P.D. & Lotey, N.K. 2015. Role of circulating tumor cells in future diagnosis and therapy of cancer. *Journal Cancer Metastasis Treat* 1: 44-56.
- Pulaski, B.A. & Ostrand-Rosenberg, S. 2001. Mouse 4T1 breast tumor model. *Current Protocols in Immunology* 20: 22.
- Rajaratnam, H., Rasudin, N.S., Al Astani, T., Mokhtar, N.F., Yahya, M.M., Zain, W., Asma-Abdullah, N. & Fuad, W. 2021. Breast cancer therapy affects the expression of antineonatal Nav1.5 antibodies in the serum of patients with breast cancer. *Oncology Letters* 21(2): 108.
- Roger, S., Besson, P. & Le Guennec, J.Y. 2003. Involvement of a novel fast inward sodium current in the invasion capacity of a breast cancer cell line. *Biochimica et Biophysica Acta* 1616(2): 107-111.
- Rook, M.B., Evers, M.M., Vos, M.A. & Bierhuizen, M.F. 2012. Biology of cardiac sodium channel Nav1.5 expression. *Cardiovascular Research* 93(1): 12-23.
- Sauter, B.V., Martinet, O., Zhang, W.J., Mandeli, J. & Woo, S.L. 2000. Adenovirus-mediated gene transfer of endostatin *in vivo* results in high level of transgene expression and inhibition of tumor growth and metastases. *Proceedings of the National Academy of Sciences of the United States of America* 97(9): 4802-4807.
- Schmittgen, T.D. & Livak, K.J. 2008. Analyzing real-time PCR data by the comparative C(T) method. *Nature Protocols* 3(6): 1101-1108.
- Stuelten, C.H., Parent, C.A. & Montell, D.J. 2018. Cell motility in cancer invasion and metastasis: Insights from simple model organisms. *Nature Reviews Cancer* 18(5): 296-312.
- Tao, K., Fang, M., Alroy, J. & Sahagian, G.G. 2008. Imagable 4T1 model for the study of late stage breast cancer. *BMC Cancer* 8: 228.
- Tsukamoto, H., Fujieda, K., Senju, S., Ikeda, T., Oshiumi, H. & Nishimura, Y. 2018. Immune-suppressive effects of interleukin-6 on T-cell-mediated anti-tumor immunity. *Cancer Science* 109(3): 523-530.
- Uddback, I.E.M., Pedersen, L.M.I., Pedersen, S.R., Steffensen, M.A., Holst, P.J., Thomsen, A.R. & Christensen, J. 2016. Combined local and systemic immunization is essential for durable T-cell mediated heterosubtypic immunity against influenza A virus. *Scientific Reports* 6: 20137.
- Yamaci, R.F., Fraser, S.P., Battaloglu, E., Kaya, H., Erguler, K., Foster, C.S. & Djamgoz, M. 2017. Neonatal Nav1.5 protein expression in normal adult human tissues and breast cancer. *Pathology, Research and Practice* 213(8): 900-907.
- Yang, M., James, A.D., Suman, R., Kasprovicz, R., Nelson, M., O'Toole, P.J. & Brackenbury, W.J. 2020. Voltage-dependent activation of Rac1 by Nav 1.5 channels promotes cell migration. *Journal of Cellular Physiology* 235(4): 3950-3972.
- Yang, M., Kozminski, D.J., Wold, L.A., Modak, R., Calhoun, J.D., Isom, L.L. & Brackenbury, W.J. 2012. Therapeutic potential for phenytoin: Targeting Na(v)1.5 sodium channels to reduce migration and invasion in metastatic breast cancer. *Breast Cancer Research and Treatment* 134(2): 603-615.
- Ye, Q., Ling, S., Zheng, S. & Xu, X. 2019. Liquid biopsy in hepatocellular carcinoma: Circulating tumor cells and circulating tumor DNA. *Molecular Cancer* 18(1): 114.

\*Corresponding author; email: wanezumi@usm.my

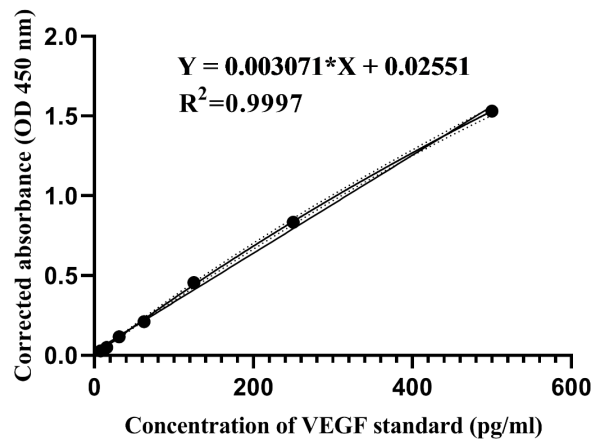


SUPPLEMENTARY FIGURE 1. The dilution of positive control sera retrieved from the positive control mice group. The decreasing expression of anti-nNav1.5-Ab in the serum of positive control mice was in accordance with the increasing ratio of dilution (Point 1-1:25, Point 2-1:50, Point 3-1:100 & Point 4-1:200)

(a)

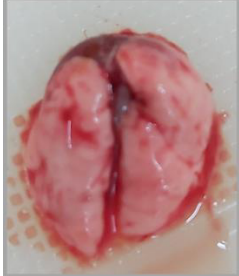
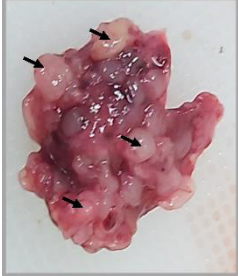
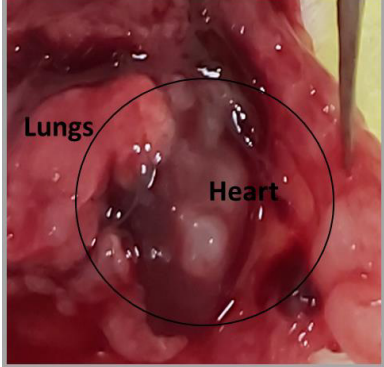


(b)



SUPPLEMENTARY FIGURE 2. The standard curves for the ELISA assays used to quantitate the concentration of IL-6 and VEGF. (a) The standard curve for the IL-6 analysis, and (b) The standard curve for the VEGF analysis

SUPPLEMENTARY TABLE 1. The gross examination of target organs resected from 4T1 orthotopic and control mice

Organ	Control mice	4T1 mice
Lungs		
	Explanation: The normal appearance of the lungs (control mice) on both sides of the lobes	Explanation: Whitish colonies (marked by the black arrows) were observed in lungs resected from 4T1 orthotopic mice
Liver		
	Explanation: The normal appearance of the liver (control mice) with intact structure	Explanation: Distortion of liver structure with whitish lesions
Spleen		
	Explanation: The normal size of a spleen retrieved from control mice.	Explanation: Spleen enlargement (splenomegaly) was observed in 4T1 mice
Heart		
	Explanation: The normal appearance of the heart	Explanation: Presence of whitish colonies on the surface of the heart

SUPPLEMENTARY TABLE 2. The absorbances (optical density) of anti-nNav1.5- Ab in each serum samples from 4T1 orthotopic and control mice groups obtained from the in-house indirect ELISA

Control (n=20)	4T1 Orthotopic (n=17)
0.000 ± 0.000	3.716 ± 0.098
0.000 ± 0.000	4.329 ± 0.260
0.169 ± 1.397	4.375 ± 0.194
1.646 ± 0.060	4.512 ± 0.000
1.331 ± 0.252	4.226 ± 0.405
1.517 ± 0.088	4.512 ± 0.001
1.370 ± 0.390	4.019 ± 0.148
1.553 ± 0.086	4.137 ± 0.075
1.639 ± 0.216	3.846 ± 0.193
1.477 ± 0.072	4.274 ± 0.337
1.801 ± 0.103	4.290 ± 0.203
1.117 ± 0.629	4.357 ± 0.220
1.253 ± 0.086	4.053 ± 0.552
1.458 ± 0.251	4.285 ± 0.322
0.762 ± 0.284	4.512 ± 0.000
0.926 ± 0.049	4.158 ± 0.142
1.257 ± 0.077	3.846 ± 0.033
0.870 ± 0.100	-
1.421 ± 0.035	-
1.651 ± 0.006	-

Note: Data expressed as mean ± SD. (Blank Absorbance: 1.488)